Particle Volume Reconstruction: Plenoptic Camera and Scanning Laser

Valerie Troutman
Stanford University
Stanford, CA
vtrout@stanford.edu

EE367 – Winter 2016
Computational Imaging and Display
Final Project Report
http://stanford.edu/class/ee367/

Abstract

A single camera, simple 3D volumetric, portable imaging system is needed to fully capture the 3D components of various fluid phenomenon in the ocean. Particle tracking within a volume of about $20 \times 20 \times 20\,\mathrm{cm}^3$ *is required to image organisms of interest. With a well constructed volume for each time step, particle tracking algorithms can be applied to ultimately produce a velocity field of the particles changing in time. The scope of this project is to understand and quantify the feasibility of using light field imaging for particle tracking through scanning the laser. This project proposes that the laser sheet is swept through the volume of interest during the exposure time of the camera. A 3D calibration tool was developed to determine the precision of the depth measurement. The projected pixel size in the image is about* $20\,\mathrm{pixels/cm}$ *and the potential depth resolution was found to be about* $0.25\,\mathrm{cm}$*. In general, the work presented here does lead to the conclusion that using a plenoptic camera does have advantages in volume capture speed and potential depth resolution, both critical performance metrics. A larger memory and computational time is required when using the plenoptic camera, but a higher volume capture speed is obtainable. About* $300\,\mathrm{particles}$ *were able to be resolved in the volume of interest, which is sufficient for particle tracking purposes.*

1. Introduction

Particle tracking velocimetry (PTV) is a technique that tracks sparse particles suspended in a fluid to better understand the characteristics of the flow. Particle image velocimetry (PIV) is a similar technique that requires a densely seeded volume. Plenoptic imaging (or light field imaging) collects the 4D light field of a scene by placing a microlens array in front of the sensor of a camera. The collected image is processed to generate multiple new images where the focus depth and perspective are different. This work aims to combine and expand these two technologies in order to determine if 3D PTV on a $20 \times 20 \times 20\,\mathrm{cm}^3$ volume using a laser, spinning mirror and a plenoptic camera is feasible. The laser sweeps through the volume of interest, illuminating the particles during the exposure time of the camera. The collected image is processed to reconstruct the volume of particles.

1.1. Motivation

A single camera, simple 3D volumetric, portable imaging system is needed to fully capture the 3D components of various fluid phenomenon in the ocean. Particle tracking within a volume of about $20 \times 20 \times 20\,\mathrm{cm}^3$ is required to image organisms of interest. With a well constructed volume for each time step, PTV algorithms can be applied to ultimately produce a velocity field of the particles changing in time.

For most physical flows, the third dimension is critical to resolve, but collecting the third dimension experimentally poses many challenges. Synchronizing multiple cameras is a common solution for this problem, but is costly and for the proposed application, very bulky. Another solution is to sweep a laser sheet through a volume, capturing multiple pictures throughout the illuminated volume. The images are combined to reconstruct the volume, but the frame rate of the camera severely limits the speed in which one can collect the full volume. Additionally, the location of the laser sheet throughout the sweeping pattern needs to be resolved in time.

Current plenoptic 3D particle work seems to be limited by the size of the volume that can be captured. The width of the laser sheet and the resolution of the plenoptic camera both are contributing factors. Also, large complicated and computationally expensive algorithms are currently used to resolve volumes collected by a plenoptic camera. A simpler calibration and image processing pipeline is ideal, but the feasibility and accuracy of such a process needs to be determined. A better understanding on the limitations of the depth resolution is desired.

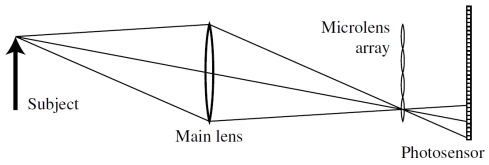

Figure 1. A conceptual schematic of the plenoptic camera developed by Ng et al. [5]

1.2. Scope

The scope of this project is to understand and quantify the feasibility of using light field imaging for particle tracking through scanning the laser. The previous particle tracking has been limited to the thickness of the laser sheet, this project aims to sweep the entire volume of interest with a thin laser sheet during the exposure time of the camera.

The main efforts include determining the resolution of the reconstructed images and the depth determination of the particles. This includes accurate calibrations for the x-, y- and z-directions. A 3D calibration tool will be developed to determine the precision of the depth measurement.

Ultimately the developed imaging diagnostic needs to be portable, therefore the amount of memory storage required is an important feature. Furthermore, the computational time and capabilities required to process the data are critical metrics to determine.

This work aims to provide a proof-of-concept for the proposed diagnostic.

2. Related Work

2.1. Plenoptic camera

A hand-held plenoptic camera was developed by Ng et al. that collects the 4D light field by placing a microlens array between the sensor and the main lens of the camera, shown in Figure 1 [5]. This work laid the foundation for the development of the Lytro Illum camera used in this project.

This configuration allows the collected image collected on the sensor to be computationally rearranged to produce multiple photos of the same scene focused at different depths. Equation 1 describes the lens equation. The distance of the sensor, S_{sensor} is computationally altered, allowing the distance of the object in focus S_{object} to also be altered (the main lens focal length f is held constant).

$$\frac{1}{f} = \frac{1}{S_{sensor}} + \frac{1}{S_{object}} \tag{1}$$

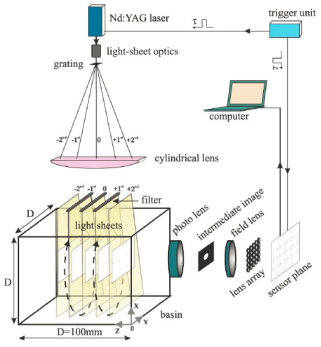

Figure 2. The imaging of 5 depth simultaneously using a plenoptic camera [6]

Figure 3. An example of the regions used to calculate the depth of the calibration plate from the Lytro depth map value [1]

2.2. Particle Image Velocimetry

3D PIV has been performed using a plenoptic camera within a volume on the millimeter scale ($67 \times 39 \times 45\,\mathrm{mm}^3$ and $61 \times 91 \times 100\,\mathrm{mm}^3$) [3]. Tomographic algorithms (MART) were used to reconstruct the volume [2, 3].

Skupsch and Brucker imaged multiple discrete planes within a volume using a light-field camera [6]. Two-dimensional PIV was then performed at those depth locations. Five planes were images within a $30 \times 30 \times 50\,\mathrm{mm}^3$ volume.

One example of work reconstructing a volume of particles via a scanning laser was done by Hori and Sakakibara. A laser light sheet was scanned by an optical scanner in a direction normal to the sheet, and two high-speed cameras captured the particle images [4]. Each volume ($100 \times 100 \times 100\,\mathrm{mm}^3$) contained 50 planes that were captured within $22\,\mathrm{s}$.

2.3. Plenoptic Calibration

Previous work has been done to calibrate the first generation Lytro camera for particle tracking [1]. The Lytro depth map algorithm was used to develop a correlation between the depth map and the physical location of the calibration plates.

Light Field Resolution	40 Megaray
Focal Length	$f = 30 - 250\,\mathrm{mm}$
Lens Aperture	$f/2.0$
Max Shutter Speed	$32\,\mathrm{s}$

Table 1. Lytro Illum Technical Specifications

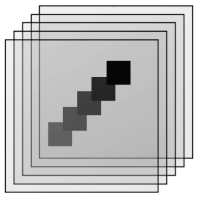

Figure 4. The configuration of the calibration plates that were stacked together

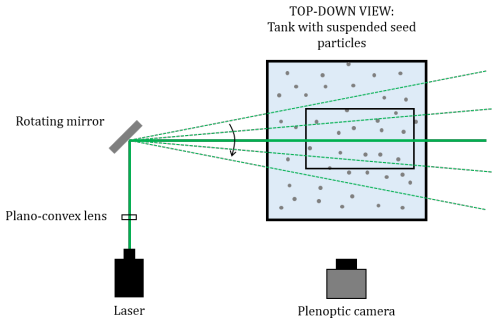

Figure 5. Scanning laser and plenoptic camera setup

Focal Length	$f = 33\,\mathrm{mm}$
Lens Aperture	$f/2.0$
Shutter Speed	$1/2\,\mathrm{s}$
ISO	160

Table 2. Lytro Illum Settings

3. Method

3.1. Lytro Illum Camera

The camera used for this work was the Lytro Illum light field camera to take single images. A few key technical specifications are detailed in Table 1

The Lytro Power Tools program was used to convert the raw Lytro file (.LFR) into a rectified image (.png). All image processing was done using MATLAB.

3.2. Calibration Setup

Seven $12 \times 12\,\mathrm{in}^2$ clear acrylic plates with a thickness of $3/32\,\mathrm{in}$ were used to build the calibration tool depicted in Figure 4. A solid square of masking tape was placed on each acrylic plate to create sharp edges.The plates were stacked flush together to create the known difference in depth location.

Additionally, $1.5 \times 1.5\,\mathrm{in}^2$ squares with a checkerboard pattern were used to build a similar calibration tool. The same acrylic plates were stacked and placed at $2\,\mathrm{in}$ increments between 10 and $20\,\mathrm{in}$ from the camera lens.

3.3. Particle Volume Experimental Setup

The setup used for this works is described by Figure 5. A LaserGlow Technologies laser emitting at $532\,\mathrm{nm}$ was guided through a plano-convex lens to form a sheet. A spinning mirror was developed to direct the sheet through the volume during the exposure time of the Lytro camera. The Lytro Illum was operated at the settings listed in Table 2.

Due to the capabilities of the Lytro Illum and the time constraints for this project, the Lytro Illum was manually triggered to capture the image as the laser was sweeping through the volume.

3.4. Depth Determination

In the rectified light field image, the pixels underneath each microlens are shifted and added together (Equation 2) to produce images at varying focal depths.

$$i_d(x) = \int_\Omega l_d(x, v), dv = \int_\Omega l_o(x - dv, v) dv \qquad (2)$$

The shifts are performed at $0.1\,\mathrm{pixel}$ increments. The gradients in both the x- and y-direction are calculated for each pixel within the refocused images. The magnitude of the gradient is normalized within each image. The pixel with the maximum gradient is utilized for calculations.

$$Gradient_{magnitude} = \sum_{channels} \sqrt{D_x^2 + D_y^2} \qquad (3)$$

For the calibration, first the location of the squares is determined. Then the magnitude of the gradients within the designated square are normalized, allowing for the gradients below 0.5 to be removed to reduce noise. Within the square of interest, the shift for that depth location is calculated by performing a weighted average. The shift values are weighted by the corresponding gradient value.

From multiple trials and combinations, it was determined that first converting the RGB light field image into HSV proved to be beneficial. Working with only the saturation channel aided in determining the sharpest gradients, and removed a majority of the background and laser artifacts. Additionally it saved significant computational time.

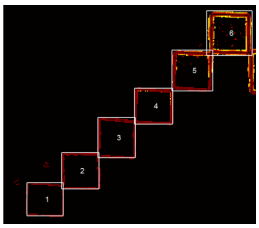

Figure 6. Example Calibration

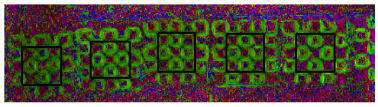

Figure 7. Example processed checkerboard image, black lines indicate the region studied

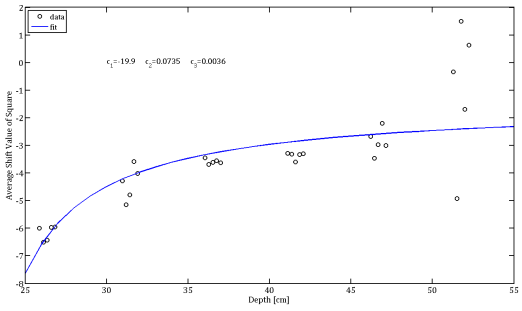

Figure 8. The calibration data and equation fit

4. Results

4.1. Calibration

The first calibration was done by using solid squares at known depth distances apart. The resulting scaled image of the shift that had the highest maximum gradient is shown in Figure 6.

The calibration tool with solid squares proved to be difficult to work with and analyze, which led to the development of a checkerboard calibration. Using the checkerboard pattern allowed for addition sharp gradients to be present at each known depth location. Figure 7 is an example of a processed calibration image.

Modeled after the lens equation, Equation 4 was used to fit the collected calibration data.

$$S_{object}[\text{cm}] = \frac{c_1}{\frac{1}{c_2} - \frac{1}{c_3 \cdot d_{shift}}} \tag{4}$$

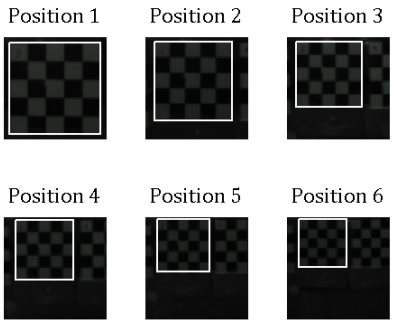

Figure 9. The same $1.5 \times 1.5\,\text{in}^2$ square is projected onto a different number of pixels depending on the depth location. A white outline has been added to highlight the size of the checkerboard in the image

4.2. Projected Pixel

The project pixel size changes with the distance from the camera lens. With a larger volume needing to be reconstructed, this cannot be neglected and must be accounted for to obtain accurate velocity measurements of the particles. The effect of depth on the projected pixel size is shown in Figure 9.

From similar triangles, a relationship between the physical size of an object (l_{object}), the projected size in the image (l_{image}) and the depth of the object (z_{object}) is shown in Equation 5. It is convenient to use an equivalent focal depth ($f_{equivalent}$) to calibrate the connection between depth and projected pixel size.

$$\frac{l_{image}[\text{pixel}]}{l_{object}[\text{cm}]} = \frac{f_{equivalent}[\text{pixel}]}{z_{object}[\text{cm}]} \tag{5}$$

An equivalent focal depth for the Lytro camera, at the experimental settings, was determined to be $f_{equivalent} = 481\,\text{pixels}$.The collected calibration data, and the best fit are shown in Figure 10.

4.3. Volume Reconstruction

A small excerpt from the processed images is shown in Figure 11. The changing shift brings the particles in and out of focus.

One way to show the depth map created from the light-field image is by weighting the view pixel by it's gradient in HSV (Figure 12). The hue represents the shift value in which the particle was most in focus, the value represents the magnitude of the gradient.

Figure 13 shows the particles from Figure 12 positioned in 3D space. The particle positions have not been calibrated,

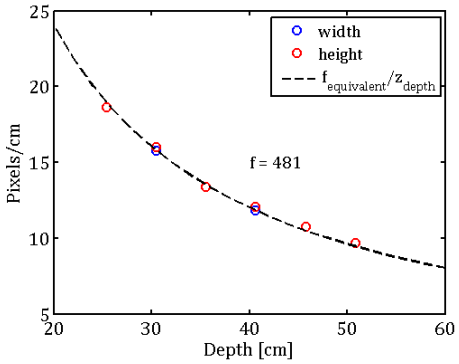

Figure 10. Best fit

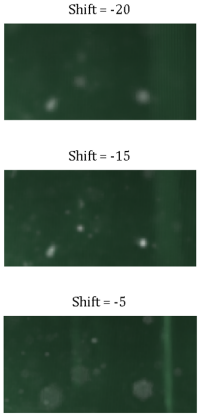

Figure 11. Example excerpt

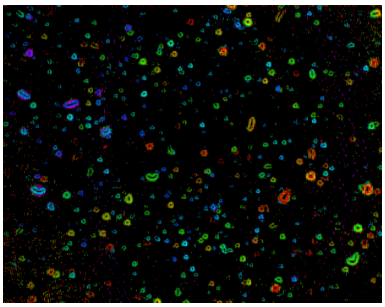

Figure 12. Example depth map, plotted using the HSV scale.

pixel and shift values are the units of the axis. With a shifted perspective, Figure 14 shows the particles in the X-Y plane.

An estimate for the calibrated volume reconstruction is shown in Figure 15 to get a better understanding of the physical volume size. This was done by scaling the pixel values by an estimated projected pixel size of $20\,\mathrm{pixels/cm}$.

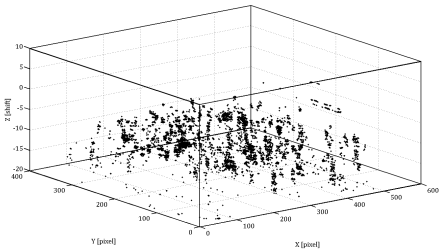

Figure 13. Example reconstructed volume

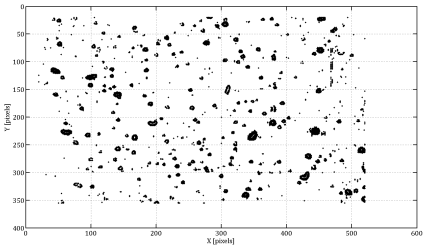

Figure 14. Example reconstructed volume, X-Y view

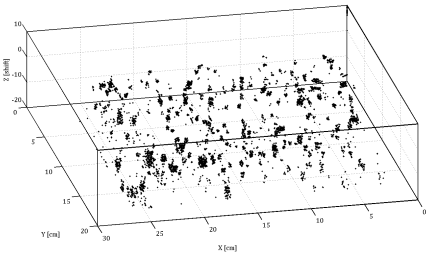

Figure 15. Example reconstructed volume, X-Y calibrated

4.4. Lytro Illum and Computational Time

In order to understand the optimal specifications required for a future plenoptic camera that can record video, the capabilities and setbacks of the Lytro Illum need to be understood. With additional time and better depth estimation algorithms, the depth resolution of the thicknesses of the acrylic sheets should be resolvable. From the checkerboard calibration, depths of up to $45\,\mathrm{cm}$ should be resolvable.

The run time for processing the three color channel of the light field image on the author's personal laptop (Lenovo T431s) averaged around $35\,\mathrm{min}$. For a $1\,\mathrm{s}$ video, at a frame rate of $30\,\mathrm{Hz}$ it would take approximately $17\,\mathrm{hr}$ to reconstruct the volumes.

Reconstructed image	$375 \times 540\,\text{pixels}$
Approx X-Y resolution	$\sim 15\,\text{pixels/cm}$
Approx X-Y area	$20 \times 30\,\text{cm}^2$
Depth resolution	$\sim 0.25\,\text{cm}$
Depth distance potential	$\sim 45\,\text{cm}$

Table 3. test table

	Plenoptic (Raytrix)
Resolution per image	$< 375 \times 540\,\text{pixels}$
Depth resolution	$\sim 0.25\,\text{cm}$
Memory per image	$250\,\text{MB}$
Memory per volume	$250\,\text{MB}$
Volume capture speed	$30 - 90\,\text{Hz}$

Table 4. Comparing the sweeping laser technique using a 4D plenoptic camera and a traditional 2D camera – Raytrix plenoptic camera

	Traditional (Emergent)
Resolution per image	$1088 \times 2048\,\text{pixels}$
Depth resolution	$\sim 0.6\,\text{cm}$
Memory per image	$4\,\text{MB}$
Memory per volume	$\sim 160\,\text{MB}$
Volume capture speed	$\sim 5 - 10\,\text{Hz}$

Table 5. Comparing the sweeping laser technique using a 4D plenoptic camera and a traditional 2D camera – Emergent Vision Technologies

4.5. Comparison to Traditional Volume Sweep

It is important to compare this proposed imaging diagnostic to the scanning laser technique that currently employed with a traditional 2D camera. A few key parameters are organized in Tables 4 and 5.

An Emergent Vision Technologies CMOS camera can be operated at around $400\,\text{fps}$. About $40\,\text{frames}$ will be required to fully resolve the volume, which brings the volume capture speed down to about $10\,\text{Hz}$. The depth resolution was estimated from assuming $40\,\text{frames}$ would be captured per volume.

Raytrix R5 high-speed lightfield camera can run at $30 - 90\,\text{fps}$. With only one image per volume, the volume capture speed is also $30 - 90\,\text{fps}$. But the resolution of the Raytrix camera may be less than the Lytro but is assumed to be similar.

5. Discussion

In general, the work presented here does lead to the conclusion that using a plenoptic camera does have advantages in volume capture speed and potential depth resolution, both critical performance metrics. A larger memory and computational time is required when using the plenoptic camera, but a higher volume capture speed is obtainable. About $300\,\text{particles}$ were able to be resolved in the volume of interest (Figure 12) which is sufficient for particle tracking purposes.

A more complicated depth determination algorithm will need to be implemented to develop this diagnostic to full capacity. The depth calibration done in this work didn't match up well with the calculated particle shift values well. This is likely due to the checkerboard calibration photos being taken on a different day than the particle volume photos. The focal length setting on the Lytro camera was held constant ($f = 33\,\text{mm}$), but other settings on the camera may have changed in between possession without the author's knowledge.

6. Future Work

Future work to continue to develop this 3D imaging diagnostic includes a more robust calibration method. The two methods presented are not satisfactory to resolve the volume of particles. The computational time necessary to process the image and build the volume can be sped up by doing the focal shift in Fourier space as well as processing images in parallel and using multiple cores.

Naturally, an additional extension to this work includes utilizing a plenoptic camera that has video capture capabilities. This will allow particle tracking to be performed on the volume of particles.

Finally, a more comprehensive depth estimation algorithm should be implemented. This will undoubtedly increase the precision of both the calibration and the volume reconstruction. One algorithm that could be implemented is combining defocus and correspondence [7].

7. Acknowledgments

The author would like to thank the EE367 course instructor Prof. Gordon Wetzstein as well as the teaching assistants Orly Liba and Liang Shi.

This work was done to fulfill the final project requirement of the Stanford University course EE367: Particle Volume Reconstruction: Plenoptic Camera and Scanning Laser.

References

[1] R. L. Bierasinski, J. D. Ellis, and D. H. Kelley. Calibration of a plenoptic camera for use in three-dimensional particle tracking by Supervised by. 2014.

[2] T. W. Fahringer and B. S. Thurow. Tomographic Reconstruction of a 3-D Flow Field Using a Plenoptic Camera. (June):1–13, 2012.

[3] T. W. Fahringer and B. S. Thurow. The Effect of Grid Resolution on the Accuracy of Tomographic Reconstruction Using a Plenoptic Camera. (January):1–12, 2013.

[4] T. Hori and J. Sakakibara. High-speed scanning stereoscopic PIV for 3D vorticity measurement in liquids. 15:1067–1078, 2004.

[5] R. Ng, M. Levoy, G. Duval, M. Horowitz, and P. Hanrahan. Light Field Photography with a Hand-held Plenoptic Camera. pages 1–11, 2005.

[6] C. Skupsch and C. Brücker. Multiple-plane particle image velocimetry using a light-field camera. 21(2):1–8, 2013.

[7] M. W. Tao, S. Hadap, J. Malik, and R. Ramamoorthi. Depth from Combining Defocus and Correspondence Using Light-Field Cameras. 2, 2013.